FTIR Spectroscopy of the Complex between *pharaonis* Phoborhodopsin and Its Transducer Protein†

Yuji Furutani,‡,§,|| Yuki Sudo,⊥ Naoki Kamo,⊥ and Hideki Kandori*,‡,||

Department of Applied Chemistry, Nagoya Institute of Technology, Showa-ku, Nagoya 466-8555, Japan, Department of Biophysics, Graduate School of Science, Kyoto University, Sakyo-ku, Kyoto 606-8502, Japan, Core Research for Evolutional Science and Technology (CREST), Japan Science and Technology Corporation, Kyoto 606-8502, Japan, and Laboratory of Biophysical Chemistry, Graduate School of Pharmaceutical Sciences, Hokkaido University, Sapporo 060-0812, Japan

Received February 25, 2003; Revised Manuscript Received March 13, 2003

ABSTRACT: *pharaonis* phoborhodopsin (*p*pR; also called *pharaonis* sensory rhodopsin II, *p*sRII) is a photoreceptor for negative phototaxis in *Natronobacterium pharaonis*. *p*pR activates the cognate transducer protein, *p*HtrII, upon absorption of light. *p*pR and *p*HtrII form a tight 2:2 complex in the unphotolyzed state, and the interaction is somehow altered during the photocycle of *p*pR. In this paper, we studied the influence of *p*HtrII on the structural changes occurring upon retinal photoisomerization in *p*pR by means of low-temperature FTIR spectroscopy. We trapped the K intermediate at 77 K and compared the ppR$_K$ minus *p*pR spectra in the absence and presence of *p*HtrII. There are no differences in the X−D stretching vibrations (2700−1900 cm^{-1}) caused by presence of *p*HtrII. This result indicates that the hydrogen-bonding network in the Schiff base region is not altered by interaction with *p*HtrII, which is consistent with the same absorption spectrum of *p*pR with or without *p*HtrII. In contrast, the ppR$_K$ minus *p*pR infrared difference spectra are clearly influenced by the presence of *p*HtrII in amide-I (1680−1640 cm^{-1}) and amide-A (3350−3250 cm^{-1}) vibrations. The identical spectra for the complex of the unlabeled *p*pR and ^{13}C- or ^{15}N-labeled *p*HtrII indicate that the observed structural changes for the peptide backbone originate from *p*pR only and are altered by retinal photoisomerization. The changes do not come from *p*HtrII, implying that the light signal is not transmitted to *p*HtrII in ppR$_K$. In addition, we observed D_2O-insensitive bands at 3479 (−)/3369 (+) cm^{-1} only in the presence of *p*HtrII, which presumably originate from an X−H stretch of an amino acid side chain inside the protein.

pharaonis phoborhodopsin (*p*pR)[1] from *Natronobacterium pharaonis* is a member of the archaeal rhodopsins family (*1*, *2*). *p*pR activates the cognate transducer protein, *p*HtrII, upon light absorption leading to negative phototaxis. It possesses a retinal chromophore that is attached to one of its 7-transmembrane helices, similarly to the case of well-studied proton-pump bacteriorhodopsin (BR) (*1*−*3*). In *p*pR and BR, the retinal forms a Schiff base linkage with Lys205 or Lys216, respectively, and the protonated Schiff base is stabilized by a negatively charged counterion, Asp75 or Asp85, respectively. Light absorption by *p*pR triggers trans−cis photoisomerization of the retinal chromophore in its electronically excited state (*4*), followed by rapid formation of the ground-state species such as the K intermediate (*5*). The same process occurs in BR also. Relaxation of the primary intermediates eventually leads to functional processes during their photocycles (*1*−*3*).

Although molecular mechanism of the *p*pR functioning is not completely understood, its functional expression in *Escherichia coli* (*6*) produced a large amount of the protein to be characterized in detail (see ref *1* for review). The crystal structure of *p*pR was determined in 2001 by two groups (*7*, *8*). The crystal structure of the K intermediate was also determined (*9*). In addition, the crystal structure of the *p*pR-*p*HtrII complex has been reported recently (Figure 1) (*10*). These advances opened the next stage of research on this photosensor.

We started comparative studies of *p*pR and BR by means of low-temperature FTIR spectroscopy. The results on the primary K intermediate revealed the structural similarity between *p*pR and BR in the polyene chain of the chromophore (*11*) and hydrogen bonds of internal water molecules (*12*). These observations were consistent with the similar crystallographic structures of *p*pR (*7*, *8*) and BR (*13*, *14*). In contrast, the K state in *p*pR after photoisomerization had larger protein structural changes than in BR (*11*, *15*), which is consistent with the recent crystallographic structure of ppR$_K$ (*9*). We also reported the ppR$_M$ minus *p*pR spectra, which showed that ppR$_M$ does not have the N-like protein structure (*16*, *17*). These low-temperature FTIR spectra are reproduced by the recent time-resolved FTIR study (*18*).

† This work was supported by grants from Japanese Ministry of Education, Culture, Sports, Science, and Technology to H.K.

* To whom correspondence should be addressed. Phone and fax: 81-52-735-5207. E-mail: kandori@ach.nitech.ac.jp.

‡ Nagoya Institute of Technology.

§ Kyoto University.

|| CREST.

⊥ Hokkaido University.

[1] Abbreviations: *p*pR, *pharaonis* phoborhodopsin; *p*HtrII, truncated *pharaonis* halobacterial transducer II expressed from 1st to 159th position; ppR$_K$, K-intermediate of *p*pR; ppR$_M$, M-intermediate of *p*pR; BR, light-adapted bacteriorhodopsin that has all-trans retinal as its chromophore; FTIR, Fourier transform infrared; DM, *n*-dodecyl-*β*-D-maltoside.

10.1021/bi034317y CCC: $25.00
Published on Web 04/09/2003

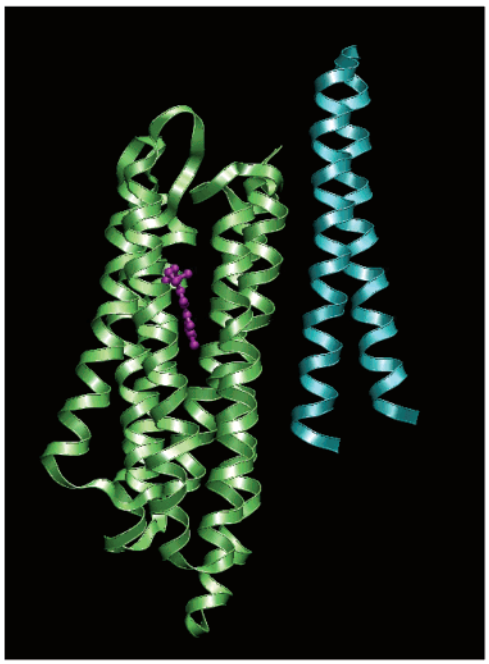

FIGURE 1: X-ray crystallographic structure of the complex between *p*pR (green) and *p*HtrII (blue) (PDB code, 1H2S) (*10*). All-trans retinal is colored purple. This figure was drawn with the program VMD (*35*).

Thus, comparative FTIR investigation of *p*pR and BR provided a number of useful results. However, the function of *p*pR is to activate the transducer protein, *p*HtrII. Therefore, the most important question in the *p*pR studies is how *p*pR transmits the light signal to *p*HtrII. To answer this question, application of FTIR spectroscopy to the complex between *p*pR and *p*HtrII is necessary and promising. We have reported the FTIR study of the complex between visual rhodopsin and a G-protein transducin (*19*, *20*). In this case, complex formation only takes place upon illumination, so the hydrated film samples in FTIR studies were not suitable, as the diffusion was a prerequisite for rhodopsin to bind transducin. In contrast, *p*pR and *p*HtrII form the 2:2 complex in the unphotolyzed state (*10*, *21*−*23*), and the complex state is stable even in a detergent such as DM (*23*). In contrast to the visual rhodopsin system, *p*HtrII is presumably locked in the inactive state by *p*pR, and activation by light corresponds to dissociation of *p*HtrII from *p*pR. Indeed, the dissociation constant is larger in ppR$_M$ than in *p*pR (*23*). EPR measurements implied light-induced tilting of the F-helix, which possibly breaks the interaction that existed in the unphotolyzed state (*22*, *24*).

Regarding the interaction mechanism of *p*pR with *p*HtrII, the recent crystallographic structure of the complex may provide an important insight since the structure of *p*pR in the complex (*10*) was very similar to that in the crystal of *p*pR itself (*7*, *8*). In fact, backbone structures are almost identical, while there are some deviations in side chains (*10*). Then, a question arises when protein structural changes (i.e., light signal) are transmitted from *p*pR to *p*HtrII. Since the photocycle of *p*pR is not much influenced by the presence of *p*HtrII (*1*), a structural study is important to provide the answer.

In this paper, we studied the influence of *p*HtrII on the structural changes occurring upon retinal photoisomerization by means of low-temperature FTIR spectroscopy. We trapped the K intermediate at 77 K and compared the ppR$_K$ minus *p*pR spectrum in the presence and absence of *p*HtrII. The ppR$_K$ minus *p*pR infrared difference spectra are clearly influenced by the presence of *p*HtrII. While there are no spectral differences in the X−D stretching vibrations (2700−1900 cm^{-1}) caused by the presence of *p*HtrII, clear differences were observed for amide-I (1680−1640 cm^{-1}) and amide-A (3350−3250 cm^{-1}) vibrations. The former result indicates that the hydrogen-bonding network in the Schiff base region is not altered by interaction with *p*HtrII, which is consistent with the fact that the absorption spectrum of *p*pR is identical with and without *p*HtrII (*23*). The latter result indicates that the complex formation affects the structure of the peptide backbone. The identical spectra for the complex of the unlabeled *p*pR and ^{13}C- or ^{15}N-labeled *p*HtrII revealed that the observed structural changes for the peptide backbone originate from *p*pR, and the light-signal is not transmitted to *p*HtrII in ppR$_K$. We also observed D_2O-insensitive bands at 3479 (−)/3369 (+) cm^{-1} only in the presence of *p*HtrII, which presumably originate from an X−H stretch of amino acid side chain inside the protein. The nature of complex formation between *p*pR and *p*HtrII is discussed on the basis of the present vibrational analysis.

MATERIALS AND METHODS

Sample Preparation. Procedure of the sample preparation was described previously (*11*, *25*, *26*), where *p*HtrII was truncated at position 159. Briefly, the *p*pR and *p*HtrII proteins possessing a histidine tag at the C-terminus were expressed in *E. coli* BL21 (DE3), solubilized with 1.5% *n*-dodecyl-*β*-D-maltoside (DM), and purified by Ni-column. The purified *p*pR and *p*HtrII proteins were mixed in the 1:1 molar ratio and incubated for 1 h at 4 °C. Complex formation was confirmed by the decay kinetics of ppR$_M$ as described (*23*). The mixture was then reconstituted into L-α-phosphatidylcholine (PC) liposomes (*p*pR/PC = 1:50 molar ratio) by removing DM by dialysis.

Uniformly ^{15}N- or ^{13}C-labeled *p*HtrII was prepared by growing cells in standard minimal medium containing 0.5 g/L ^{15}N-ammonium chloride (Isotec Inc.) or 1 g/L ^{13}C-D-glucose (Isotec Inc.), respectively.

FTIR Spectroscopy. FTIR spectroscopy was performed as described previously (*11*, *12*). The *p*pR sample in the PC liposomes was washed twice by a buffer at pH 7 (2 mM phosphate). A total of 90 μL of the *p*pR sample was dried on a BaF_2 window with a diameter of 18 mm. After hydration by either H_2O or D_2O, the sample was placed in a cell, which was mounted in an Oxford DN-1704 cryostat mounted in the Bio-Rad FTS-40 spectrometer. Illumination conditions for *p*pR were identical to those reported previously; 450 nm light for *p*pR to ppR$_K$ conversion and >560 nm light for the ppR$_K$ to *p*pR conversion at 77 K (*11*). The difference spectrum was calculated from the spectra constructed with 128 interferograms before and after the illumination. Twenty-four spectra obtained in this way were averaged for the ppR$_K$ minus *p*pR.

We measured the spectra from two independent preparations (different expressions). In each preparation, two films were made, and spectra were compared. All these samples produced the same results. In addition, we also measured

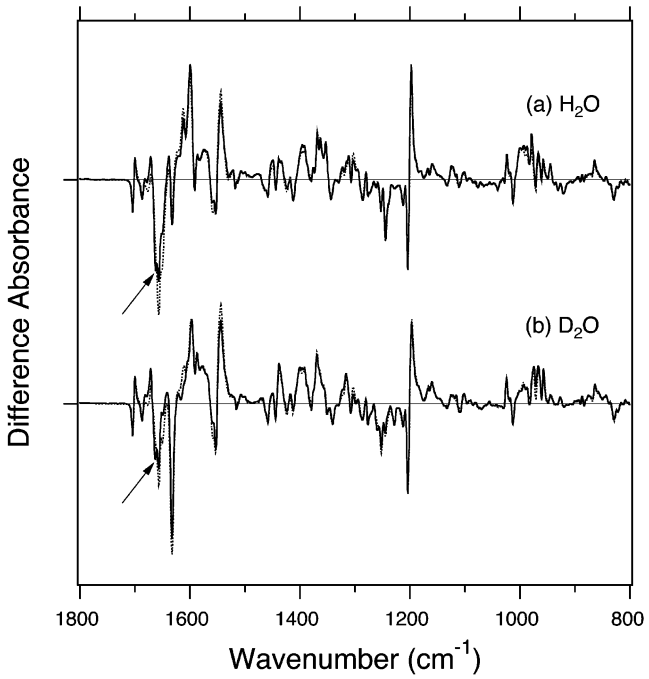

FIGURE 2: *p*pR$_K$ minus *p*pR infrared difference spectra in the absence (dotted line) and presence (solid line) of the transducer protein, *p*HtrII, in the 1800−800 cm^{-1} region. Spectra are measured at 77 K and pH 7 upon hydration with H_2O (a) and D_2O (b). The spectra look very similar with and without *p*HtrII, while a spectral difference is seen in the frequency region of amide-I vibration (arrows).

the spectra of the 1:2 mixture of *p*pR and *p*HtrII, whose spectra were identical to the 1:1 mixture.

RESULTS

Spectral Differences Caused by Presence of pHtrII in Vibrations in the Low-Frequency Region. Figure 2 shows *p*pR$_K$ minus *p*pR infrared difference spectra in the absence (dotted line) and presence (solid line) of *p*HtrII in the 1800−800 cm^{-1} region. Both dotted and solid lines look very similar in this frequency region, indicating that the complex formation between *p*pR and *p*HtrII has almost no effect on the structural alterations that happen upon the retinal photoisomerization. Nevertheless, a spectral difference was observed in the frequency region of amide-I vibration (arrows).

Figure 3 expands the data of Figure 2 in the 1710−1615 cm^{-1} region. There are two negative peaks at 1657 and 1651 cm^{-1} in the absence of *p*HtrII (dotted line in Figure 3a). These frequencies are characteristic of amide-I vibration of α-helix. The C═N stretching vibration of the retinal Schiff base is also located in this frequency region. In fact, a broad negative feature in the 1660−1650 cm^{-1} region in H_2O (dotted line in Figure 3a) is reduced in D_2O (dotted line in Figure 3b), by shifting to 1633 cm^{-1}. In the presence of *p*HtrII, new negative and positive peaks appear at 1663 and 1671 cm^{-1}, respectively, in H_2O, while negative peaks at 1657 and 1651 cm^{-1} are reduced in amplitude (Figure 3a). These observations are repeated in D_2O, although the peaks at 1671 (+)/1663 (−) cm^{-1} seem to exist even in the absence of *p*HtrII (Figure 3b). The 1704 (−)/1700 (+) cm^{-1} bands, which were assigned to the C═O stretching vibration of Asn105 (*15*), are never influenced by the presence of *p*HtrII.

The 1671 (+)/1663 (−) cm^{-1} bands appear in the frequency region typical for the amide-I vibration of the α_{II}-helix, while the 1657 cm^{-1} band appears in the range of amide-I vibration of the α_I-helix (*27*). Since the α_{II}-helix possesses considerably distorted structure (*28*), the present observation suggests that the association of *p*pR and *p*HtrII yields distortion of the helical structure that is altered by the retinal photoisomerization.

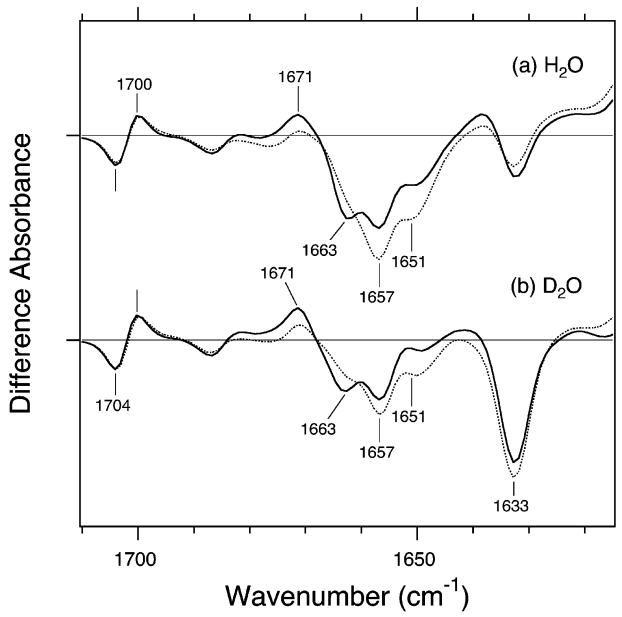

FIGURE 3: *p*pR$_K$ minus *p*pR infrared difference spectra in the absence (dotted line) and presence (solid line) of the transducer protein, *p*HtrII. The spectra in Figure 2 are enlarged to show the 1710−1615 cm^{-1} region clearly.

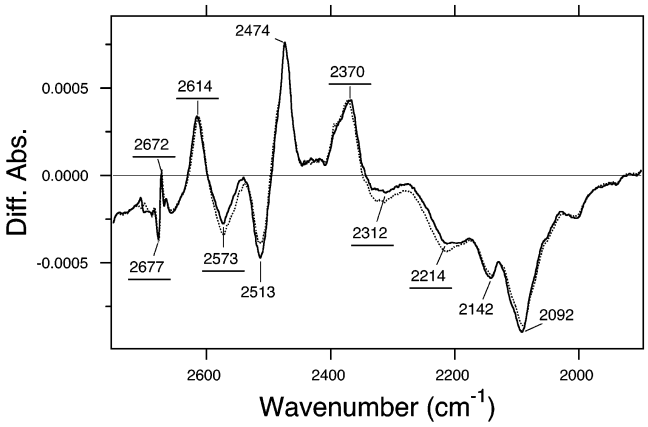

FIGURE 4: *p*pR$_K$ minus *p*pR infrared difference spectra in the absence (dotted line) and presence (solid line) of the transducer protein, *p*HtrII, in the 2750−1900 cm^{-1} region. Spectra are measured at 77 K and pH 7 upon hydration with D_2O.

Spectral Differences Caused by Presence of pHtrII in X−D Stretching Vibrations. Figure 4 shows *p*pR$_K$ minus *p*pR infrared difference spectra in the absence (dotted line) and presence (solid line) of *p*HtrII in the 2750−1900 cm^{-1} region. Both spectra coincide well in this frequency region, implying that there is no influence of the transducer protein. Previous spectral comparison between hydration with D_2O and $D_2{}^{18}O$ demonstrated the isotope shift of water molecules at 2677 (−), 2672 (+), 2614 (+), 2573 (−), 2370 (+), 2312 (−), and 2214 (−) cm^{-1} (*12*, *29*). The peaks at 2513 (−)/2474 (+) cm^{-1} did not exhibit the isotope shift of water molecules (*12*, *29*). Since a similar phenomenon was observed for the 2506 (−)/2466 (+) cm^{-1} bands of Thr89 in BR (*30*), they

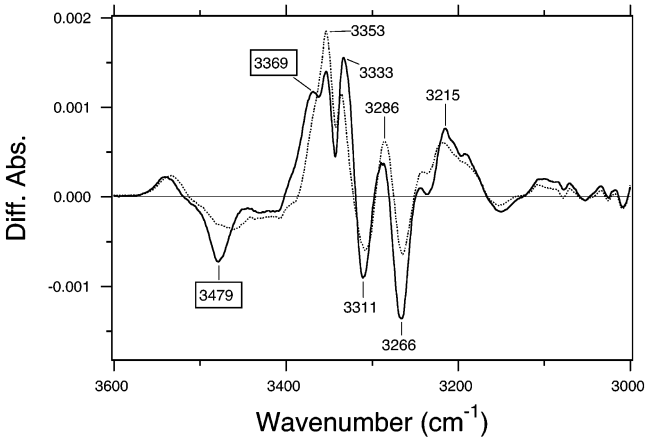

FIGURE 5: *p*ppR$_K$ minus *p*pR infrared difference spectra in the absence (dotted line) and presence (solid line) of the transducer protein, *p*HtrII, in the 3600−3000 cm^{-1} region. Spectra are measured at 77 K and pH 7 upon hydration with D_2O.

possibly originate from the O−D stretch of Thr79. Negative peaks at 2142 and 2092 cm^{-1} do not originate from the water O−D stretches (*12*, *29*). Since the N−D stretch of the retinal Schiff base in BR is located at similar frequencies (*31*), they possibly originate from the N−D stretch of the retinal Schiff base. Thus, spectral changes in the X−D stretching vibrations are direct probes of hydrogen-bonding alterations in the Schiff base region, and two coincident spectra suggest that the complex formation does not affect the structure of the hydrogen-bonding network present in the retinal Schiff base region. This observation is consistent with the fact that the complex formation does not change the color of *p*pR.

Spectral Differences Caused by Presence of pHtrII for X−H Stretching Vibrations. The N−H stretching vibrations of the peptide backbone (amide-A) appear at 3320−3270 cm^{-1}, where amide-A vibration of the α-helix is located at 3279 cm^{-1} (*27*). Therefore, the sharp peaks at 3333 (+), 3311 (−), 3286 (+), and 3266 (−) cm^{-1} in D_2O (Figure 5) probably correspond to amide-A vibrations. As described above, peaks at 1671 (+), 1663 (−), and 1657 (−) cm^{-1} (Figure 2) are attributable to amide-I vibrations (*28*). Since the frequency at 1657 cm^{-1} corresponds to characteristic amide-I vibration of an ideal α-helix, the N−H group with a vibration at 3266 cm^{-1} is likely to form hydrogen bond with the C═O group with vibration at 1657 cm^{-1} in *p*pR. On the other hand, it is known that amide-A and amide-I vibrations are considerably upshifted in the distorted α-helix, α_{II}-helix (*28*). Thus, the amide-A vibrations at 3333 (+)/3311 (−) cm^{-1} are likely to correspond to the amide-I vibrations at 1671 (+)/1662 (−) cm^{-1}, which probe structural changes in the α_{II}-helix. The frequency upshift of the α_{II}-helix upon formation of *p*pR$_K$ indicates weakened hydrogen bonding. This observation is in contrast to that for BR, where frequency downshifts were observed for both amide-A and amide-I vibrations of the α_{II}-helix (*32*).

There are spectral differences in the amide-A region caused by the presence of *p*HtrII (Figure 5). As is the case of amide-I vibration, the bands of the amide-A vibration of α_{II}-helix (3333 (+)/3311 (−) cm^{-1}) increase their intensities in the presence of *p*HtrII. In addition, a clear difference was observed in the higher frequency region. Figure 5 shows the negative 3479 cm^{-1} and positive 3369 cm^{-1} bands only in the presence of *p*HtrII. These frequencies are considerably higher than the amide-A vibrations. Therefore, either the N−H or the O−H stretching vibration of an amino acid side chain is likely to undergo hydrogen-bonding alteration upon retinal photoisomerization. This group is H−D unexchangeable, and it seems that the hydrogen bond is strengthened so as to exhibit frequency downshift by about 100 cm^{-1}.

Effect of Isotope Substitution in pHtrII on the ppR$_K$ Minus ppR Difference Spectra. The *p*pR$_K$ minus *p*pR infrared difference spectra are clearly influenced by the presence of *p*HtrII. While there are no spectral changes for the X−D stretching vibrations caused by the presence of *p*HtrII (Figure 4), such spectral changes were observed for amide-I (Figure 3) and amide-A (Figure 5) vibrations. In addition, new bands appeared at 3479 (−)/3369 (+) cm^{-1} in the presence of *p*HtrII (Figure 5). These facts indicate the structural perturbation by *p*HtrII. In particular, the spectral changes in amide-I and amide-A vibrations indicate perturbation of the peptide backbone. Then, a question arises as to whether these bands originate from vibrations of *p*pR or *p*HtrII. In the former case, the interaction of *p*HtrII and *p*pR changes the structure of *p*pR, which is altered upon retinal photoisomerization. The latter case means that the protein structural changes caused by retinal photoisomerization are already transmitted to the transducer protein in the K state. Since the K formation takes place in picoseconds, the latter case may indicate ultrafast signal transduction from the receptor to the transducer protein.

The complex is formed from independently expressed *p*pR and *p*HtrII proteins. Therefore, we are able to examine the above-mentioned question by using isotope labeling of one of the two proteins. In the present study, we expressed *p*HtrII protein in either ^{13}C- or ^{15}N-enriched medium and produced its complex with the unlabeled *p*pR. As a consequence, the complex possesses the unlabeled *p*pR and either ^{13}C- or ^{15}N-labeled *p*HtrII proteins. If we detect isotope-induced spectral shifts, we can conclude that the new bands observed for the complex originate from vibrations of *p*HtrII.

Figure 6 shows spectral comparison of the *p*pR$_K$ minus *p*pR infrared difference spectra in the presence of isotope-labeled (solid lines) and unlabeled (dotted lines) *p*HtrII. Since the normal mode of amide-I vibration corresponds to the C═O stretch of the peptide backbone, we compared the unlabeled and ^{13}C-labeled *p*HtrII in Figure 6a. If the band originates from the amide-I vibration of *p*HtrII, we expect to see the isotope-induced spectral downshift by about 30−40 cm^{-1}. No such downshift was observed in Figure 6a, although some spectral deviations were observed in the 1670−1650 and 1600−1570 cm^{-1} regions. Therefore, we concluded that the bands do not contain vibrations of *p*HtrII. No isotope shift was observed for ^{15}N-labeled *p*HtrII in this frequency region (data not shown).

Since the normal mode of amide-A vibration corresponds to the N−H stretch of the peptide backbone, we compared the unlabeled and ^{15}N-labeled *p*HtrII in Figure 6b. If the band originates from the amide-A vibration of *p*HtrII, we expect to see the isotope-induced spectral downshift by about 10 cm^{-1}. No such downshift was observed in Figure 6b, indicating that the bands do not contain vibrations of *p*HtrII. No isotope shift was observed for ^{13}C-labeled *p*HtrII in this frequency region (data not shown).

By use of isotope label of *p*HtrII, we excluded the possibility that the light-signal is transmitted from *p*pR to

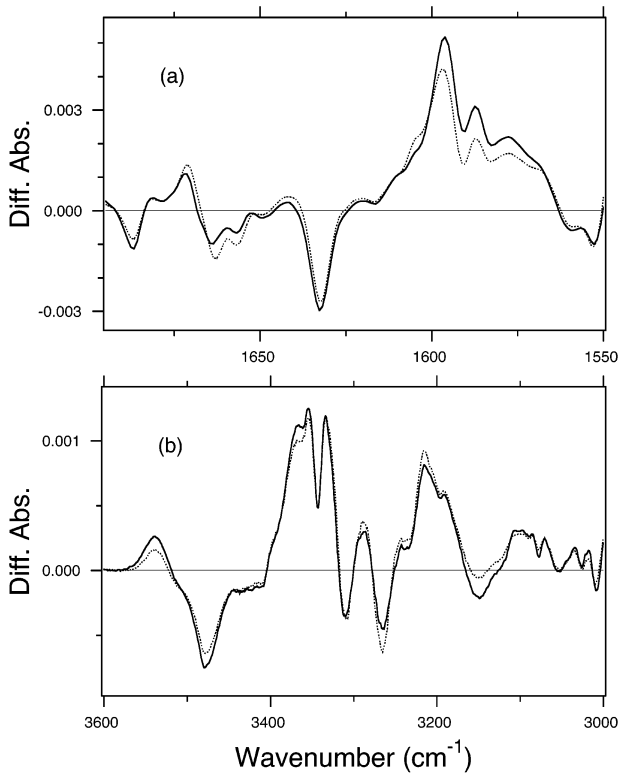

FIGURE 6: *p*pR$_K$ minus *p*pR infrared difference spectra in the presence of the transducer protein, *p*HtrII, where *p*HtrII is ^{13}C-labeled (solid line in a), ^{15}N-labeled (solid line in b), or unlabeled (dotted lines in a and b). Spectra are measured at 77 K and pH 7 upon hydration with D_2O.

*p*HtrII in the K intermediate. It should be noted that we did not use ^{18}O isotope label in this study, so that the O−H stretching frequency of *p*HtrII may be involved in the observed change. On the other hand, we concluded that the peptide backbone alterations observed in this study originate from *p*pR, not from *p*HtrII. Association with *p*HtrII leads to an alteration of the peptide backbone structure of *p*pR, which is involved in the structural changes upon retinal photoisomerization.

DISCUSSION

In this paper, we studied the influence of *p*HtrII on the structural changes occurring upon retinal photoisomerization in *p*pR by means of low-temperature FTIR spectroscopy. We trapped the K intermediate at 77 K and compared the *p*pR$_K$ minus *p*pR spectra with and without *p*HtrII. There are no spectral changes for the X−D stretching vibrations (2700−1900 cm^{-1}) caused by presence of *p*HtrII, indicating that the hydrogen-bonding network in the Schiff base region is not altered by interaction with *p*HtrII. The result is consistent with the same absorption spectra of *p*pR with and without *p*HtrII. These features are in contrast to those of sensory rhodopsin (sR; also called sensory rhodopsin I, sRI), where complex formation with the transducer protein changes the pK_a of the counterion of the Schiff base (*33*).

The *p*pR$_K$ minus *p*pR infrared difference spectra are clearly affected by the presence of *p*HtrII in amide-I (1680−1640 cm^{-1}) and amide-A (3350−3250 cm^{-1}) vibrations. The identical spectra for the complex of the unlabeled *p*pR and ^{13}C- or ^{15}N-labeled *p*HtrII indicate that the observed structural changes for the peptide backbone originate from *p*pR. The recent X-ray crystallographic structure of the complex between *p*pR and *p*HtrII with 1.94 Å resolution (*10*) showed the identical peptide backbone structure of *p*pR in the absence and presence of *p*HtrII (*7*, *8*). This observation does not necessarily contradict the present FTIR results because of the difference in resolution. Krimm and Bandekar showed the linear relationship between the amide-A frequency and the distance from the nitrogen to the oxygen atom, when the oxygen is the hydrogen-bonding acceptor (*27*). According to the relationship, the variation corresponds to 0.0035 Å/cm^{-1}. Therefore, if amide-A frequency shifts by 10 cm^{-1}, the hydrogen bond of the peptide backbone can be shortened by 0.035 Å. Thus, the present FTIR study probably detects the structural perturbations of the peptide backbone in *p*pR upon the transducer binding, which are much smaller than the X-ray detection limit. Influence of *p*HtrII on the peptide backbone structure has been also reported by solid-state NMR (*34*).

Beside the signal from peptide backbone, we observed the bands at 3479 (−)/3369 (+) cm^{-1} appearing in the presence of *p*HtrII. Since the X−H group is not deuterated in D_2O, it is likely to be buried inside the protein. It is also possible that the X−H group is located at the surface between *p*pR and *p*HtrII. According to the crystal structure of the complex (*10*), Tyr199 of *p*pR forms a hydrogen bond with Asn74 of *p*HtrII in the middle of membrane, while Thr189 of *p*pR forms hydrogen bonds with Glu43 and Ser62 of *p*HtrII at the cytoplasmic side. Tyr199 is indeed important for the interaction with *p*HtrII (*26*). Identification of the X−H group is our future focus.

In conclusion, the present study is the first report of the IR difference spectra of *p*pR in the presence of its transducer protein, *p*HtrII, to study the mechanism of light-signal transduction in archaeal rhodopsins. Unlike in visual rhodopsins, *p*pR forms a complex with *p*HtrII in its unphotolyzed state. The influence of *p*HtrII was observed for the primary photointermediate, *p*pR$_K$, which is trapped at 77 K. Such perturbation does not originate from the ultrafast signal transduction. Rather, structural modification of *p*pR by *p*HtrII was concluded from the measurements with isotopically labeled *p*HtrII. Thus, taken together with our previous studies on visual rhodopsin (*19*, *20*), this work demonstrated that FTIR spectroscopy can provide useful information about molecular mechanism of rhodopsins at the atomic resolution.

ACKNOWLEDGMENT

We thank Drs. K. Shimono and M. Iwamoto for valuable discussions.

REFERENCES

1. Kamo, N., Shimono, K., Iwamoto, M., and Sudo, Y. (2001) *Biochemistry (Moscow) 66*, 1277−1282.
2. Sasaki, J., and Spudich, J. L. (2000) *Biochim. Biophys. Acta 1460*, 230−239.
3. Spudich, J. L., and Lanyi, J. K. (1996) *Curr. Opin. Cell Biol. 8*, 452−457.
4. Kandori, H., Tomioka, H., and Sasabe, H. (2002) *J. Phys. Chem. A 106*, 2091−2095.
5. Lutz, I., Sieg, A., Wegener, A. A., Engelhard, M., Boche, I., Otsuka, M., Oesterhelt, D., Wachtveitl, J., and Zinth, W. (2001) *Proc. Natl. Acad. Sci. U.S.A. 98*, 962−967.
6. Shimono, K., Iwamoto, M., Sumi, M., and Kamo, N. (1997) *FEBS Lett. 420*, 54−56.

7. Luecke, H., Schobert, B., Lanyi, J. K., Spudich, E. N., and Spudich, J. L. (2001) *Science 293*, 1499−1503.
8. Royant, A., Nollert, P., Edman, K., Neutze, R., Landau, E. M., Pebay-Peyroula, E., and Navarro, J. (2001) *Proc. Natl. Acad. Sci. U.S.A. 98*, 10131−10136.
9. Edman, K., Royant, A., Nollert, P., Maxwell, C. A., Pebay-Peyroula, E., Navarro, J., Neutze, R., and Landau, E. M. (2002) *Structure 10*, 473−482.
10. Gordeliy, V. I., Labahn, J., Moukhametzianov, R., Efremov, R., Granzin, J., Schlesinger, R., Büldt, G., Savopol, T., Scheidig, A. J., Klare, J. P., and Engelhard, M. (2002) *Nature 419*, 484−487.
11. Kandori, H., Shimono, K., Sudo, Y., Iwamoto, M., Shichida, Y., and Kamo, N. (2001) *Biochemistry 40*, 9238−9246.
12. Kandori, H., Furutani, Y., Shimono, K., Shichida, Y., and Kamo, N. (2001) *Biochemistry 40*, 15693−15698.
13. Luecke, H., Schobert, B., Richter, H.-T., Cartailler, J. P., and Lanyi, J. K. (1999) *J. Mol. Biol. 291*, 899−911.
14. Belrhali, H., Nollert, P., Royant, A., Menzel, C., Rosenbusch, J. P., Landau, E. M., and Pebay-Peyroula, E. (1999) *Structure Fold Des. 15*, 909−917.
15. Kandori, H., Shimono, K., Shichida, Y., and Kamo, N. (2002) *Biochemistry 41*, 4554−4559.
16. Furutani, Y., Iwamoto, M., Shimono, K., Kamo, N., and Kandori, H. (2002) *Biophys. J. 83*, 3482−3489.
17. Iwamoto, M., Furutani, Y., Kamo, N., and Kandori, H. (2003) *Biochemistry 42*, 2790−2796.
18. Hein, M., Wegener, A. A., Engelhard, M., and Siebert, F. (2003) *Biophys. J. 84*, 1208−1217.
19. Nishimura, S., Sasaki, J., Kandori, H., Matsuda, T., Fukada, Y., and Maeda, A. (1996) *Biochemistry 35*, 13267−13271.
20. Nishimura, S., Kandori, H., and Maeda, A. (1998) *Biochemistry 37*, 15816−15824.
21. Zhang, X.-N., Zhu, J., and Spudich, J. L. (1999) *Proc. Natl. Acad. Sci. U.S.A. 96*, 857−862.
22. Wegener, A. A., Klare, J. P., Engelhard, M., and Steinhoff, H. J. (2001) *EMBO J. 20*, 5312−5319.
23. Sudo, Y., Iwamoto, M., Shimono, K., and Kamo, N. (2001) *Photochem. Photobiol. 74*, 489−494.
24. Wegener, A. A., Chizhov, I., Engelhard, M., and Steinhoff, H. J. (2000) *J. Mol. Biol. 301*, 881−891.
25. Sudo, Y., Iwamoto, M., Shimono, K., and Kamo, N. (2001) *Biochim. Biophys. Acta 1558*, 63−69.
26. Sudo, Y., Iwamoto, M., Shimono, K., and Kamo, N. (2001) *Biophys. J. 83*, 427−432.
27. Krimm, S., and Bandekar, J. (1986) *Adv. Protein Chem. 38*, 183-
28. Krimm, S., and Dwivedi, A. M. (1982) *Science 216*, 407−408.
29. Furutani, Y., and Kandori, H. (2002) *Mol. Membr. Biol. 19*, 257−265.
30. Kandori, H., Kinoshita, N., Yamazaki, Y., Maeda, A., Shichida, Y., Needleman, R., Lanyi, J. K., Bizounok, M., Herzfeld, J., Raap, J., and Lugtenburg, J. (1999) *Biochemistry 38*, 9676−9683.
31. Kandori, H., Belenky, M., and Herzfeld, J. (2002) *Biochemistry 41*, 6026−6031.
32. Kandori, H., Kinoshita, N., Maeda, A., and Shichida, Y. (1998) *J. Phys. Chem. B 102*, 7899−7905.
33. Bogomolni, R. A., Stoeckenius, W., Szundi, I., Perozo, E., Olson, K. D., and Spudich, J. L. (1994) *Proc. Natl. Acad. Sci. U.S.A. 91*, 10188−10192.
34. Arakawa, T., Shimono, K., Yamaguchi, S., Tuzi, S., Sudo, Y., Kamo, N., and Saitô, H. (2003) *FEBS Lett. 536*, 237−240.
35. Humphrey, W. F., Dalke, A., and Schulten, K. (1996) *J. Mol. Graphics 14*, 33−38.

BI034317Y